Interactions of Glutathione Tripeptide with Gold Cluster: Influence of Intramolecular Hydrogen Bond on Complexation Behavior

DATASET · FEBRUARY 2013

4 AUTHORS, INCLUDING:

Zahra Aliakbar Tehrani
Sharif University of Technology
25 PUBLICATIONS **103** CITATIONS
SEE PROFILE

Zahra Jamshidi
Chemistry & Chemical Engineering Research C…
34 PUBLICATIONS **203** CITATIONS
SEE PROFILE

Marjan Jebeli Javan
Sharif University of Technology
24 PUBLICATIONS **59** CITATIONS
SEE PROFILE

THE JOURNAL OF PHYSICAL CHEMISTRY A

Article

pubs.acs.org/JPCA

Interactions of Glutathione Tripeptide with Gold Cluster: Influence of Intramolecular Hydrogen Bond on Complexation Behavior

Zahra Aliakbar Tehrani,[†] Zahra Jamshidi,*[,‡] Marjan Jebeli Javan,[†] and Alireza Fattahi*[,†]

[†]Department of Chemistry, Sharif University of Technology, P .O. Box 11365-9516, Tehran, Iran

[‡]Chemistry and Chemical Engineering Research Center of Iran, P.O. Box 14335-186, Tehran, Iran

Supporting Information

ABSTRACT: Understanding the nature of the interaction between metal nanoparticles and biomolecules has been important in the development and design of sensors. In this paper, structural, electronic, and bonding properties of the neutral and anionic forms of glutathione tripeptide (GSH) complexes with a Au_3 cluster were studied using the DFT-B3LYP with 6-31+G**-LANL2DZ mixed basis set. Binding of glutathione with the gold cluster is governed by two different kinds of interactions: Au−X (X = N, O, and S) anchoring bond and Au···H−X nonconventional hydrogen bonding. The influence of the intramolecular hydrogen bonding of glutathione on the interaction of this peptide with the gold cluster has been investigated. To gain insight on the role of intramolecular hydrogen bonding on Au−GSH interaction, we compared interaction energies of Au−GSH complexes with those of cystein and glycine components. Our results demonstrated that, in spite of the ability of cystein to form highly stable metal−sulfide interaction, complexation behavior of glutathione is governed by its intramolecular backbone hydrogen bonding. The quantum theory of atom in molecule (QTAIM) and natural bond orbital analysis (NBO) have also been applied to interpret the nature of interactions in Au−GSH complexes. Finally, conformational flexibility of glutathione during complexation with the Au_3 cluster was investigated by means of monitoring Ramachandran angles.

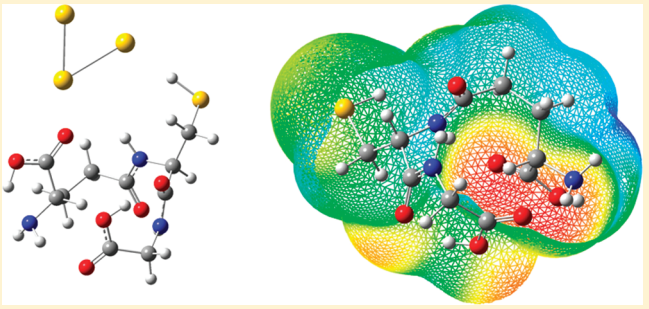

1. INTRODUCTION

The study of the interactions between biologically relevant molecules and nanoparticles has attracted increasing interest because of potential applications in sensors, biosensors, and biomedical diagnostics.[1−7] Among various nanoparticles, gold nanoparticles have attracted much attention in chemistry and material science because of their good biocompatibility, facile synthesis,[8] and conjugation to a variety of bimolecular ligands. Zhong et al. reported the detection of thiol containing amino acids such as homocysteine and cysteine using gold nanoparticles.[9] Thomas et al.[10] have reported a novel strategy for the selective detection of micromolar concentrations of cysteine and glutathione by exploiting the interplasmon coupling in Au nanorods.

Glutathione is a tripeptide (γ-glutamyl-cysteinyl-glycine, Figure 1) widely distributed peptide in biological cells.[11−13] Glutathione (GSH) is an unusual peptide with a peptide bond between the amine group of cysteine and the carboxylic group of the glutamic acid side chain. GSH has various physiological functions and is the most abundant nonprotein thiol in mammalian cells.[14] Glutathione also plays an important role in detoxification of cells and is responsible for removing harmful organic peroxides and free radicals. It binds to toxins, such as heavy metals, solvents and pesticides and transforms them into a form that can be excreted in urine or bile.[15]

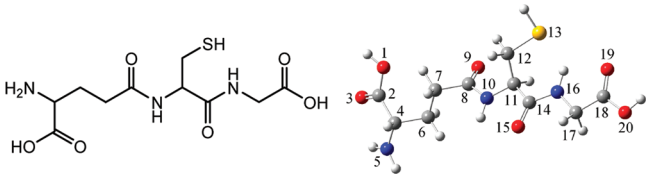

Figure 1. Chemical structure and atom numbering of gutathione (GSH).

GSH consists of the glutamate moiety with a pK_a of 2.05 for the carboxylic group and a pK_a of 9.49 for the amine group; the carboxylic group on the glycine moiety has a pK_a of 3.40 and the thiol moiety on the cysteine has a pK_a of 8.72.[15−18] The influence of pH on the interaction between Au nanoparticles and amino acids was investigated by Zhong[9] et al. Due to the presence of various functional groups, different charged species are available for GSH as result of pH changes. Consequently, presence of numerous potential metal binding sites with very different hard−soft properties (carboxylates, amine, and thiolate) makes several possible interparticle interactions for GSH with a range of transition metals.[19,20]

Received: August 20, 2011
Revised: February 18, 2012
Published: February 22, 2012

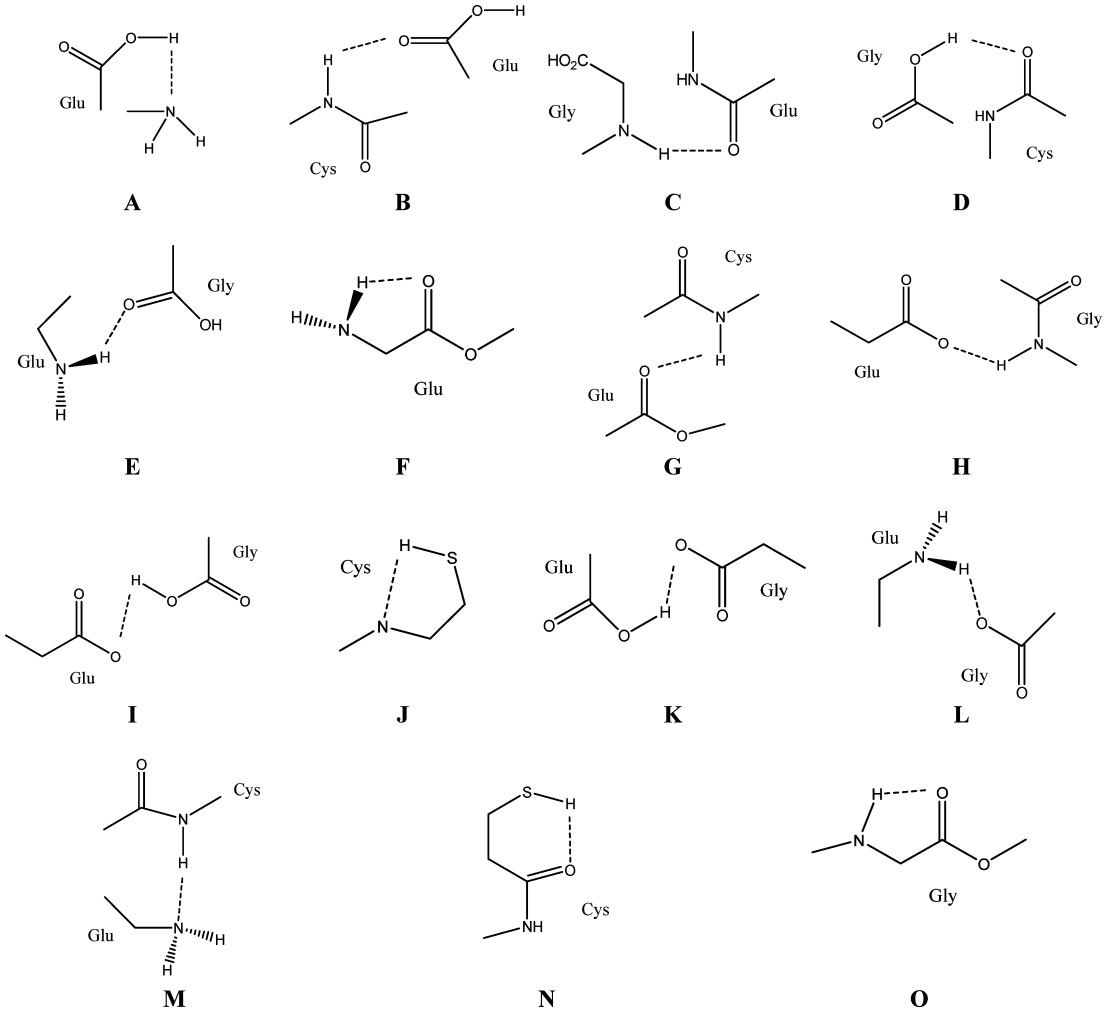

Figure 2. Hydrogen bonding types between amino, carboxyl, and thiol functional groups of a peptide backbone for neutral and anionic GSH complexes with a Au_3 cluster.

Many studies have recently been performed to understand the reactivity of glutathione in the presence of metal nanoparticles.[21−33,15] GSH−modified gold nanosurfaces were considered for specific protein binging. Ligand exchange between the GSH-Au nanoparticles with thiolated oligonucleotides has been examined by Kornbery and co-workers.[26] The self-assembly of glutathione films on gold electrode surfaces has been shown to exhibit ion-gating properties, which are useful for the selective detection of specific metal cations.[31,32] Recently, the development of a nanoparticle-based drug delivery and release system using GSH as the releasing agent has been shown to be viable.[28]

However, interparticle interactions of glutathione and metal particles remain elusive. To probe such interactions, we have investigated theoretically the interaction of neutral and anionic forms of glutathione with the Au_3 cluster, which serves as a simple catalytic model of gold nanoparticles. Interactions of the individual components of glutathione tripeptide (i.e., cystein and glycine amino acids) with the gold trimer have been compared with glutathione−Au_3 interaction to gain insight on the role of these residues and intramolecular hydrogen bonding on glutathione−Au_3 interactions. Natural bond orbital (NBO) and quantum theory of atoms in molecule (QTAIM) were also used to interpret the nature of the interaction of gold nanoparticles with glutathione. Based on the positive value of $\nabla^2\rho(r)$ and the negative value of $H(r)$ for the Au−X bond, interaction of the Au_3 cluster with the active site of the GSH ligand (Au−X, X = N, O, S) is partially covalent and partially electrostatic. However, the positive values of both $\nabla^2\rho(r)$ and $H(r)$ indicate that Au···H−X interaction of the Au_3 cluster with the GSH ligand is electrostatic in nature.

2. METHOD OF CALCULATIONS

Geometries of glutathione complexes in their neutral and anionic forms with the Au_3 cluster were fully optimized using density functional theory (DFT) calculations with a nonlocal hybrid B3LYP method[34,35] employing the Spartan program.[36] The 6-31+G** basis set was used for the atoms in GSH, while for the gold cluster the Los Alamos effective-core potential (ECP) Lanl2DZ basis set was applied.[37] The harmonic vibrational frequencies (real frequencies) and corresponding zero point vibrational energies (ZPVE) were calculated for all optimized geometries. The binding energy E_b of the complex Au_3−GSH is defined in a standard way as the absolute value of the energy difference $E_b = E_{Au3-GSH} - (E_{Au3} + E_{GSH})$ and its ZPVE-corrected values are reported throughout this work. Natural bond orbital (NBO)[38,39] and quantum theory of atoms in molecules (QTAIM)[40] analysis were carried out on optimized structures to reveal the nature of bonds. In addition, the electron density ($\rho(r)$) and its Laplacian ($\nabla^2\rho(r)$) at bond

dx.doi.org/10.1021/jp2080226 | J. Phys. Chem. A 2012, 116, 4338−4347

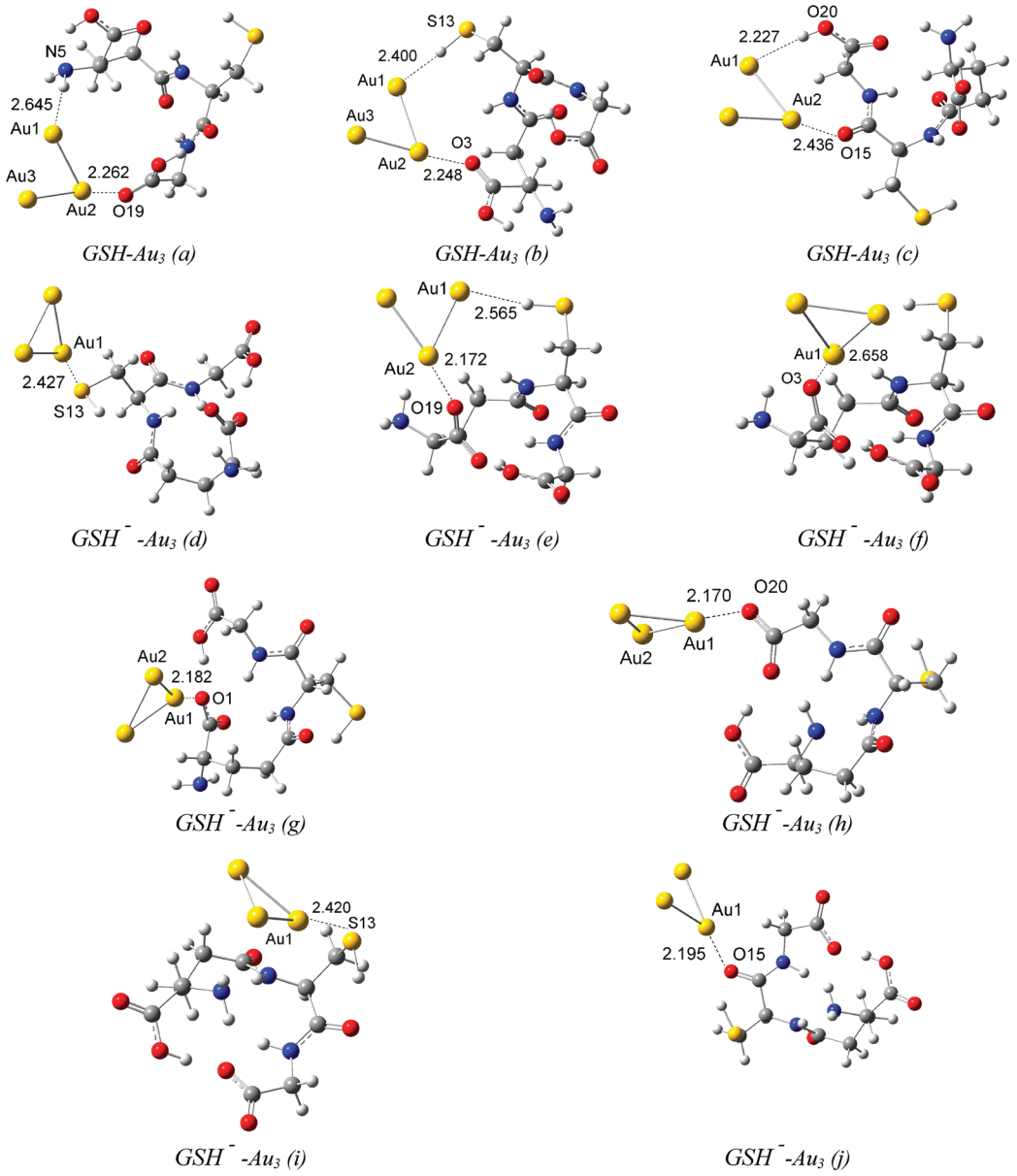

Figure 3. Optimized geometries of neural and anionic (GSH^-—Au_3(d)/(e)/(f)/(g) complexes produced by deprotonation of carboxylic acid group of Glu and GSH^-—Au_3(h)/(i)/(j) complexes produced by deprotonation of the carboxylic acid group of Gly) GSH complexes with the Au_3 cluster. Distances are reported in angstroms.

critical points (BCPs) were computed based on Bader's QTAIM using the AIM2000 package.[41]

3. RESULTS AND DISCUSSION

3.1. Structure and Energetic of GHS—Au_3 Complexes.

The starting geometries of neutral and two anionic complexes (produced by deprotonation of carboxylic acid groups of Glu or Gly moieties) were generated by placing the Au_3 cluster near the electron-rich sites of GSH (such as nitrogen, oxygen, and sulfur atoms). These sites can donate electron density via their lone pairs to the 5d and 6s orbitals of gold atoms.

The noncovalent interactions between a partially charged backbone and side chain in amino acids play an essential role in determining their stable conformers.[42] GSH is a flexible molecule and its conformational behavior is influenced by forming intramolecular hydrogen bonding, its charge, and the environment. In GSH—Au_3 complexes, intramolecular hydrogen bonds in the GSH backbone can be classified into different A to O groups, as shown in Figure 2. The B3LYP/6-31+G** U Lanl2DZ optimized structures of neutral and anionic complexes of GSH molecules with complexes of Au_3 clusters are shown in Figure 3. Moreover, geometrical features, including hydrogen bond type and its length, interaction bond lengths (r_{X-Au}), and binding energies (E_b) for neutral and anionic complexes of GSH with Au_3 clusters are collected in Table 1.

As shown in Figure 3, in the GSH—Au_3(a) complex, the gold cluster has bidentate interaction through nonconventional hydrogen bond with the amine group of Glu moiety ($N_5H_5\cdots Au_1$ = 2.645 Å) and the carboxylic group of Gly moiety (Au_2—O_{19} = 2.262 Å). In the GSH—Au_3(b) complex, GSH interacts with gold trimer through SH group of Cys moiety and carboxyl group of Glu and yields anchoring O_2—Au_2 and nonconventional $Au_1\cdots H_{13}$—S_{13} bonds with the corresponding bond lengths 2.248 and 2.400 Å, respectively.

dx.doi.org/10.1021/jp2080226 | J. Phys. Chem. A 2012, 116, 4338—4347

Table 1. Geometrical Features of Neutral and Anionic Complexes of GSH with a Au_3 Cluster

complex	r(X–Au)[a]	type of hydrogen bond and bond length	E_b[b]
GSH–Au_3(a)	S_{13}–H_{13}···Au_1 (2.400)	A (1.782), B (2.380), C (1.942), D (1.736), E (2.200)	−1.7
	O_3–Au_2 (2.248)		
GSH–Au_3(b)	N_5H_3···Au_1 (2.645)	A (1.834), B (1.903), C (1.875), D (1.612)	−3.0
	$O_{19}Au_2$ (2.262)		
GSH–Au_3(c)	O_9–Au_2 (2.436)	A (1.831), B (1.950), C (1.890), E (2.454)	−1.1
	S_{13}–Au_1 (2.427)		
GSH^-–Au_3(d)	O_3–Au_1 (2.182)	F (2.272), G (1.884), H (1.942), I (1.603), J (2.681)	−13.9
GSH^-–Au_3(e)	O_3–Au_1 (2.182)	F (2.311), G (2.048), H (2.107), I (1.791), J (2.747)	−12.2
	O_1–H_1···Au_2 (2.671)		
GSH^-–Au_3(f)	S_{13}–H_{13}···Au_2 (2.565)	F (2.747), G (2.489), H (2.019), I (1.690)	−12.8
	O_1–Au_2 (2.172)		
GSH^-–Au_3(g)	O_1–Au_1 (2.161)	F (2.435), G (2.496), H (2.000), I (1.734)	−12.3
GSH^-–Au_3(h)	O_{15}–Au_1 (2.195)	K (1.579), L (1.995), M (2.032), O (1.952)	−8.4
GSH^-–Au_3(i)	O_{20}–Au_1 (2.170)	K (1.740), L (2.005), M (2.011), N (2.600), O (2.333)	−15.7
GSH^-–Au_3(j)	S_{13}–Au_1 (2.420)	K (1.576), L (1.961), M (1.886), N (2.065), O (2.065)	−14.0

[a] r(X–Au) is the length of the anchoring bond or nonconventional H-bonds, (X = O, N, S, and H). [b] The binding energy, E_b, in kcal/mol.

The intramolecular hydrogen bonding for both GSH–Au_3(a) and GSH–Au_3(b) complexes are similar (see Table 1 for hydrogen bonding pattern).

In GSH–Au_3(c), the intramolecular hydrogen bonding network of GSH is rearranged form D-type hydrogen bond to E-type as seen in Table 1. Consequently, the hydroxyl group of the Gly moiety can participate in an interaction of GSH with the Au_3 cluster. In this structure, GSH interacts with the gold cluster through nonconventional hydrogen bond (O_1–H_1···Au_1 = 2.227 Å) and oxygen anchoring bond (O_9–Au_2 = 2.436 Å).

The recent study of the adsorption of GSH on the gold surface demonstrates that hydrogen bonding between the adsorbed GSH is dependent on pH. In a basic environment, one of the carboxylic groups of GSH deprotonates and forms an additional anchor to the gold surface.[43] Here, we decided to investigate the influence of deprotonation of the carboxylic groups form Gly and Glu moieties on intramolecular hydrogen bonding of GSH and interaction of GSH with gold cluster. As shown in Figure 3, in complexes GSH^-–Au_3(d), GSH^-–Au_3(e), GSH^-–Au_3(f), and GSH^-–Au_3(g) deprotonation of GSH occurred through the carboxylic group of Glu, while in structures GSH^-–Au_3(h), GSH^-–Au_3(i), and GSH^-–Au_3(j) deprotonation of GSH occurred through carboxylic group of Gly moiety.

In GSH^-–Au_3(d), two carboxylic arms of GSH approaching each other with I-type intramolecular hydrogen bonds with bond length of 1.603 Å (see Table 1). As a result of this folding, the anionic form of GSH has a monodendate anchoring interaction through a thiol group of the Cys moiety (S_{13}···Au_1 = 2.427 Å). As demonstrated in Table 1, the generation of a J-type intramolecular hydrogen bond between thiol and amine groups of the Cys moiety facilitates interaction of the Au_3 cluster with Gly and Glu carboxylic ends of GSH. As shown in Figure 3, for GSH^-–Au_3(g), the Au_3 cluster interacts with Gly and Glu carboxylic ends via two O_3–Au_1 = 2.182 and O_1–H_1···Au_1 = 2.671 Å bonds. Comparison of the structure of GSH^-–Au_3(d) and GSH^-–Au_3(g) with that of GSH^-–Au_3(e) demonstrates that the GSH^-–Au_3(e) complex has the combinational behavior of both of these complexes in intramolecular hydrogen pattern and coordination mode to the Au_3 cluster (see Table 1 and Figure 3 for more details). In this complex, the gold cluster interacts with the Cys moiety through a nonconventional hydrogen bond S_{13}–H_{13}···Au_2 (2.565 Å) and with the Glu moiety via an anchoring Au_2–O_1 bond (2.172 Å). In the GSH^-–Au_3(f) complex, only a short anchoring Au_1–O_3 bond (2.161 Å) can stabilize the interaction of the GSH ligand with the Au_3 cluster, and the hydrogen bonding pattern of this complex is the same as the GSH^-–Au_3(e) complex.

As shown in Figure 3, deprotonation of carboxylic group at Gly moiety cannot significantly influence on complexation behavior of GSH in comparison with that of carboxylic group of Glu moiety. Deprotonation of carboxylic group of Gly moiety forms L-type intramolecular hydrogen bonding between Gly and Glu moieties (with bond length of 1.576–1.739 Å). Consequently, as mentioned, the Au_3 cluster can interact with groups oriented outside of GSH ligand. In GSH^-–Au_3(j) and GSH^-–Au_3(h) complexes, Au–O anchoring bonds with bond lengths of Au_1–O_{15} = 2.195 Å and Au_1–O_{20} = 2.170 Å have been observed, respectively. However, in the GSH^-–Au_3(h) complex, the O-type hydrogen bonding interaction between the thiol group and the peptide bond of the Cys moiety can facilitate interaction of the Au_3 cluster with the carboxylate moiety of Gly. The GSH^-–Au_3(i) has the same complexation behavior as the GSH^-–Au_3(d) and monodendate Au_1–S_{13} interaction with a bond length of 2.420 Å.

On the other hand, Pakiari and Jamshidi previously reported[43] a binding affinity of gold and silver clusters with neutral, anionic, and cationic forms of Gly and Cys amino acids. According to their results, the average affinities of Cys to Au_3 clusters are 14.2, 45.4, and 8.5 kcal/mol for neutral, anionic, and cationic forms of Cys, respectively. In the case of Gly, their results indicate that the average affinities of neutral, anionic, and cationic forms Gly to Au_3 are 15.8, 44.0, and 7.4 kcal/mol, respectively. A comparison of these results with those of neutral and anionic forms of glutathione to Au_3 (see Table 1) indicated that complexation behaviors of Cys and Gly amino acids in this tripeptide significantly differ from those of their free forms. The glutathione has a low tendency to interact with a Au_3 cluster, and complexation behavior of glutathione is governed by its intramolecular backbone hydrogen bonding rather than intermolecular hydrogen bonds with the gold cluster.

3.2. Conformational Analysis of GSH Complexes with Au_3 Cluster in Terms of Dihedral Angles Distributions.

The biological function of amino acids, peptides, and proteins strongly depends on the conformation that the molecule adopts. Conformational flexibility of these molecules is determined by distribution of charged and polar groups in the molecule. In the gas phase, the number of available conformers is severely curtailed by intramolecular columbic repulsion or attraction and the possibility or lack of intramolecular hydrogen bond formation. Conformational

dx.doi.org/10.1021/jp2080226 | J. Phys. Chem. A 2012, 116, 4338–4347

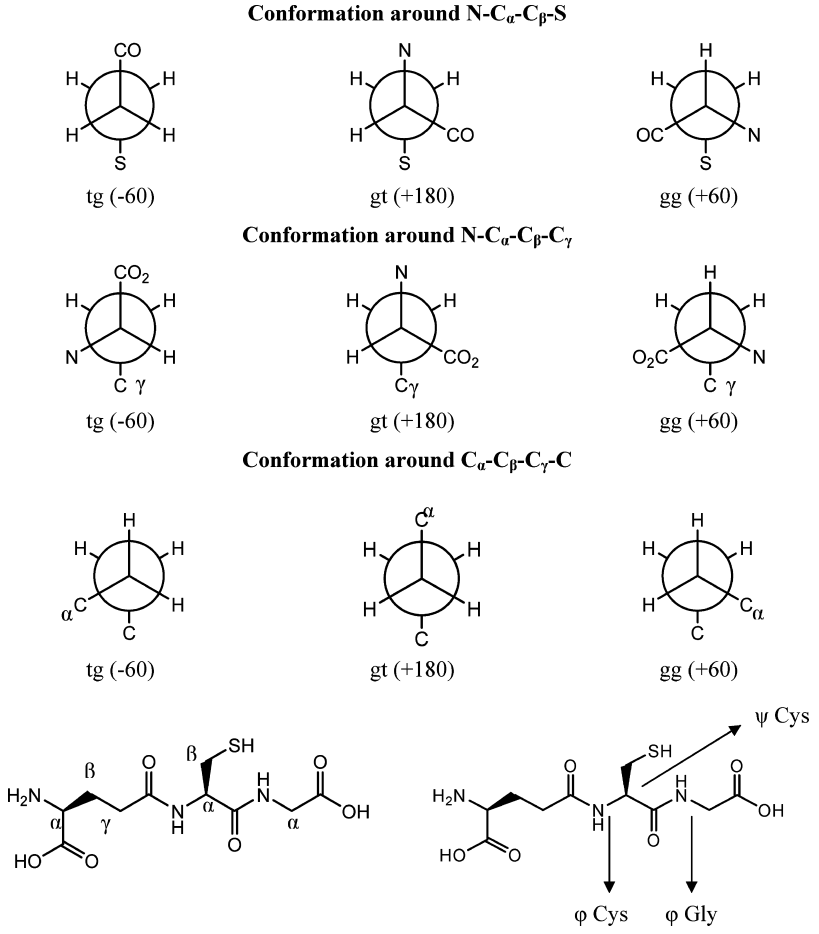

Figure 4. Definition of dihedral angles of neutral and anionic complexes of GSH with a Au_3 cluster.

Table 2. Dihedral Angles of the Neutral and Anionic Complexes of GSH with a Au_3 Cluster

complexes	N−C_α−C_β−S	N−C_α−C_β−C_γ	C_α−C_β−C_γ−C	φ Cys	Ψ Cys	φ Gly	backbone type
GSH−Au_3(a)	−69.2	+170.5	+63.9	+95.6	−110.4	−107.5	δ_D
GSH−Au_3(b)	−61.8	−176.0	+57.2	+94.2	−101.4	−92.8	δ_D
GSH−Au_3(c)	−69.0	−178.9	+57.5	+90.5	−113.9	−89.3	δ_D
GSH^-−Au_3(d)	−67.8	+64.3	+100.9	+64.7	−174.3	−65.2	ε_D
GSH^-−Au_3(e)	−68.1	+74.8	+101.2	+90.9	+179.7	−67.6	ε_D
GSH^-−Au_3(f)	−68.4	+72.5	+108.7	+84.2	+178.1	−67.6	ε_D
GSH^-−Au_3(g)	−67.1	+64.0	+102.0	+71.4	−173.8	−75.1	ε_D
GSH^-−Au_3(h)	+62.9	−65.9	+100.3	+56.9	−155.3	−20.3	δ_D
GSH^-−Au_3(i)	+73.7	−64.9	+98.4	+35.5	−139.8	−15.5	ε_D
GSH^-−Au_3(j)	+63.6	−63.3	+102.1	+63.9	−168.1	−8.9	ε_D

flexibility of GSH during complexation with the Au_3 cluster can be determined by the monitoring of some dihedral angles. As seen in Figure 4, the side chain angles N−C_α−C_β−S of Cys and the two backbone angles N−C_α−C_β−C_γ and C_α−C_β−C_γ−C in the Glu moiety are defined as the Ramachandran angles of the cysteine moiety (φ Cys and ψ Cys) and the glycine moiety (φ Gly).

Newman projection of the N−C_α−C_β−S angle of the cysteinyl moiety (Figure 4) indicates that +60° rotamer corresponds to the highly most crowded gauche−gauche conformer, while at +180° (gauche−trans) and −60° (trans−gauche) rotamers, the backbone amide N or C are in a less-crowded position anti to the S atom. Perusal of the distribution function for this angle in Table 2 reveals that the −60° rotamer is favored in GSH−Au_3(a), GSH−Au_3(b), GSH^-−Au_3(d), GSH^-−Au_3(e), GSH^-−Au_3(f), and GSH^-−Au_3(g) complexes. This situation is dramatically reversed in the case of GSH^-−Au_3(h), GSH^-−Au_3(i), and GSH^-−Au_3(j) complexes, where the N−C_α−C_β−S angle of the cysteinyl moiety has "gauche−gauche" rotamers. In these complexes, the S atom forms a hydrogen bond with the N−H bond of the cysteinyl moiety (see Table 1 for more details).

Similar considerations apply to the N−C_α−C_β−C_γ dihedral angle of the glutamyl moiety. The most hindered rotamer, +60° or gauche−gauche rotamer with all gauche interactions of the large groups, is populated at GSH^-−Au_3(d), GSH^-−Au_3(e), and GSH^-−Au_3(f) and GSH^-−Au_3(g) complexes. Steric hindrance of this rotamer is compensated by formation of an intramolecular hydrogen bond between negatively charged glutamyl carboxyl group and the N−H bond of the proximal

dx.doi.org/10.1021/jp2080226 | J. Phys. Chem. A 2012, 116, 4338−4347

amide group (see Tables 1 and 2 for more details). The C_α–C_β–C_γ–C dihedral angle of the glutamyl moiety is not as hindered. The most stable form should be at +180° in which the distal C atoms are anti to one another. It is worth mentioning that the gauche forms have an appreciable population in complexes of neutral and anionic complexes of GSH with a Au_3 cluster due to intramolecular hydrogen bond formation in these complexes.

Figure 5 shows, in a schematic way, the idealized topology of the backbone conformational potential energy surface (PES) of

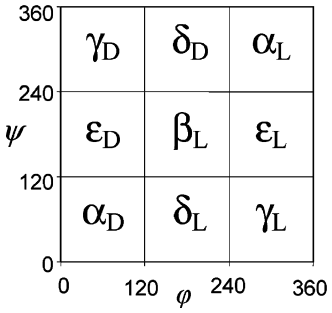

Figure 5. Topological representation of the Ramachandran or backbone map showing two Ψ and φ full cycles of rotation.

an amino acid residue. Two full cycles, $-180° \leq \Psi \leq +180°$ and $-180° \leq \varphi \leq +180°$, of rotation are shown. Most amino acids exhibit nine unique conformations labeled as γ_D, δ_D, α_D, α_L, β_L, ε_L, γ_L, and δ_L (see Figure 5 for more details). These notations are applied to describe alternative backbone conformers for all neutral and anionic complexes of GSH with a Au_3 cluster. Comparison of the backbone conformation of neutral and anionic complexes of GSH with a Au_3 cluster suggest that the δ_D backbone conformations are observed in GSH–Au_3(a), GSH–Au_3(b), GSH–Au_3(c), and GSH–Au_3(h) complexes. However, ε_D backbone conformations are observed in GSH^-–Au_3(d), GSH^-–Au_3(e), GSH^-–Au_3(f), GSH^-–Au_3(g), GSH^-–Au_3(j), and GSH^-–Au_3(i) complexes (see Table 2 for more details).

3.3. Atoms in Molecules Analysis. Bader's QTAIM approach provides a powerful method to analyze electron delocalization. AIM theory can also be used to probe the distinction between agostic interaction and hydrogen bonds. In AIM analysis, the nature of the bonding interaction is analyzed in terms of properties of electron density and its derivatives.

Laplacian of $\rho(r)$ is related to the bond interaction energy by a local expression of virial theorem.[44] A positive value of $\nabla^2\rho(r)$ shows a depletion of electronic charge along the bond path. This is the case in all closed-shell electrostatic interactions. A negative value of $\nabla^2\rho(r)$, on the other hand, indicates that electronic charge is concentrated in the internuclear region. This is the case in an electron-sharing (or covalent) interaction. The electronic energy density $H(r)$ at bond critical point (BCP) is defined as $H(r) = G(r) + V(r)$, where $G(r)$ and $V(r)$ correspond to the kinetic and potential energy densities, respectively.[45] The sign of $H(r)$ will depend on which contribution, potential or kinetic, will locally prevail on the BCP. $H(r) < 0$ reflects a prevalence of the potential energy, which is a consequence of the stabilization of the accumulated electron charge, a typical feature of covalent interactions. Koch and Popelier[46] proposed both $\nabla^2\rho(r) > 0$ and $H(r) > 0$ for weak and medium hydrogen bonds; $\nabla^2\rho(r) > 0$ and $H(r) < 0$ for strong hydrogen bonds, whereas for very strong hydrogen bonds both have negative values ($\nabla^2\rho(r) < 0$ and $H(r) < 0$). The latter are usually classified as covalent in nature. This classification shows that weak hydrogen bonds eventually merge with (weaker) van der Waals interactions, whereas strong hydrogen bonds merge, at the other end of the continuum, with covalent and polar bonds.

Tables 3–5 show values for electron densities $\rho(r)$ and their Laplacians $\nabla^2\rho(r)$, kinetic energy densities $G(r)$, potential energy densities $V(r)$, and electronic energy densities $H(r)$ at the BCPs of various intramolecular hydrogen bond and Au-X bonds (where X is N, O, S, and H atoms) for neutral and anionic complexes of GSH with Au_3 cluster. It has been indicated very often that the electron density at BCP is a good measure of bonding strength. Popelier[44,46] proposed a set of rules to demarcate the hydrogen bonded and agostic systems. According to these rules, $\rho(r)$ lies between 0.002 and 0.035 a.u. for a hydrogen-bonded system, whereas for an agostic system, $\rho(r)$ lies outside this range. Furthermore, $\nabla^2\rho(r)$ lies between 0.024 and 0.139 a.u. for the hydrogen-bonded system and 0.150–0.250 for an agostic case. As shown in Tables 3–5, for all complexes, most of $\rho(r)$ values of hydrogen bonds are within this range. The rest of them are in excess of the range, which indicates that a partial covalent character is attributed to these hydrogen bonds. Furthermore, the shorter H···X bond distance

Table 3. Bond Critical Point Data (in a.u.) from AIM Analysis for Neutral Complexes of GSH with a Au_3 Cluster

complexes	BCP	$\rho(r)$	$\nabla^2\rho(r)$	$G(r)$	$V(r)$	$H(r)$
GSH–Au_3(a)	N_5H_5–O_{19}	0.048	0.111	0.032	−0.036	−0.004
	O_1H_1–N_5	0.015	0.046	0.011	−0.011	0.001
	$O_{20}H_{20}$–O_{15}	0.041	0.121	0.031	−0.031	−0.001
	$N_{16}H_{16}$–O_9	0.027	0.082	0.021	−0.021	0.000
	$N_{10}H_{10}$–O_3	0.012	0.034	0.009	−0.010	−0.001
GSH–Au_3(b)	N_5–Au_1	0.013	0.034	0.008	−0.008	0.001
	$O_{20}H_{20}$–O_{15}	0.056	0.150	0.042	−0.046	−0.004
	O_1–H_1–N_5	0.042	0.107	0.030	−0.032	−0.003
	$N_{10}H_{10}$–O_3	0.029	0.084	0.021	−0.022	0.000
	N_{16}–H_{16}–O_9	0.032	0.092	0.023	−0.024	−0.001
GSH–Au_3(c)	O_1H_1–N_5	0.043	0.107	0.030	−0.033	−0.003
	N_5H_5–O_{19}	0.008	0.033	0.007	−0.006	0.001
	$N_{16}H_{16}$–O_{19}	0.030	0.088	0.023	−0.023	0.000
	$N_{10}H_{10}$–O_3	0.027	0.071	0.020	−0.021	−0.002

dx.doi.org/10.1021/jp2080226 | J. Phys. Chem. A 2012, 116, 4338–4347

Table 4. Bond Critical Point Data (in a.u.) from AIM Analysis of Anionic Complexes of GSH with a Au_3 Cluster[a]

complexes	BCP	$\rho(r)$	$\nabla^2\rho(r)$	$G(r)$	$V(r)$	$H(r)$
GSH^--Au_3(d)	$N_5H_5-O_1$	0.018	0.075	0.017	−0.014	0.002
	$N_{10}-H_{10}-O_1$	0.030	0.084	0.022	−0.023	−0.001
	$O_{20}H_{20}-O_3$	0.057	0.149	0.042	−0.046	−0.004
	$N_{16}H_{16}-O_3$	0.028	0.079	0.021	−0.022	−0.001
	$S_{13}H_{13}-O_9$	0.015	0.050	0.013	−0.014	−0.001
GSH^--Au_3(e)	$O_{20}H_{20}-O_3$	0.036	0.103	0.026	−0.026	0.000
	$N_{10}H_{10}O_1$	0.021	0.058	0.016	−0.017	−0.001
	$N_{16}H_{16}-O_3$	0.020	0.059	0.015	−0.016	0.000
	$N_5H_5-O_1$	0.021	0.058	0.016	−0.017	−0.001
	$S_{13}H_{13}-N_{10}$	0.047	−0.036	0.015	−0.038	−0.023
GSH^--Au_3(f)	$S_{13}H_{13}-Au_1$	0.025	0.014	0.009	−0.015	−0.006
	$N_5H_5-Au^2$	0.017	0.054	0.013	−0.012	0.001
	O_1-Au_2	0.076	0.374	0.099	−0.105	−0.006
	$O_{20}H_{20}-O_3$	0.045	0.130	0.033	−0.033	0.000
	$N_{16}H_{16}-O_3$	0.023	0.069	0.018	−0.018	0.000
	$N_{10}H_{10}-O_1$	0.010	0.029	0.007	−0.007	0.000
GSH^--Au_3(g)	O_1-Au_1	0.078	0.391	0.104	−0.110	−0.006
	$N_{16}H_{16}-O_3$	0.023	0.073	0.018	−0.018	0.000
	$O_4H_4-O_3$	0.037	0.119	0.029	−0.027	0.001
	$N_5H_5-O_1$	0.010	0.026	0.007	−0.008	−0.001

[a]Deprotonation of the carboxylic group from the Glu moiety.

Table 5. Bond Critical Point Data (in a.u.) from AIM Analysis of Anionic Complexes of GSH with a Au_3 Cluster[a]

complexes	BCP	$\rho(r)$	$\nabla^2\rho(r)$	$G(r)$	$V(r)$	$H(r)$
GSH^--Au_3(h)	$O_{15}-Au_1$	0.071	0.359	0.094	−0.099	−0.005
	$O_1H_1-O_{19}$	0.059	0.155	0.044	−0.049	−0.005
	$N_5H_5-O_{19}$	0.024	0.073	0.019	−0.019	−0.001
	$N_{16}H_{16}-O_9$	0.031	0.105	0.026	0.031	0.000
	$S_{13}H_{13}-O_{15}$	0.085	0.198	0.086	−0.122	−0.036
	$N_{10}H_{10}-O_3$	0.028	0.063	0.018	−0.020	−0.002
GSH^--Au_3(i)	$N_{16}H_{16}-O_9$	0.019	0.081	0.018	−0.016	0.002
	$S_{13}H_{13}-O_{15}$	0.047	−0.036	0.015	0.023	−0.023
	$N_{10}H_{10}-N_5$	0.028	0.063	0.018	0.002	−0.002
	$O_1H_1-O_{19}$	0.037	0.120	0.028	−0.002	0.002
	$N_5H_5-O_{19}$	0.023	0.070	0.018	−0.018	0.000
	$N_{16}H_{16}-O_{19}$	0.019	0.081	0.018	−0.016	0.002
GSH^--Au_3(j)	$S_{13}-Au_1$	0.080	0.192	0.071	−0.093	−0.023
	$N_5H_5-Au_3$	0.005	0.016	0.003	−0.002	0.001
	$N_{1o}-Au_1$	0.008	0.021	0.005	−0.004	0.001
	$S_{13}-H_{13}-O_{15}$	0.217	−0.604	0.041	−0.232	−0.192
	$N_5H_5-O_{19}$	0.027	0.078	0.020	−0.021	0.001
	$O_1H_1-O_{19}$	0.059	0.157	0.044	0.059	−0.005
	$N_{10}H_{10}-N_5$	0.025	0.092	0.022	−0.021	−0.022

[a]Deprotonation of the carboxylic group from the Gly moiety.

corresponds to the stronger hydrogen bond, which is characterized by a greater electron density at the corresponding BCP.

However, in the case of anchoring Au−X (X = N, O, S) and nonconventional hydrogen bonds Au···H−X (X = N, O, S), the positive value of $\nabla^2\rho(r)$ implies depletion of electronic charge along the bond, which indicates a closed shell electrostatic interaction. The sign of $H(r)$ at the BCPs of these bonds is negative for Au−X bond but positive for nonconventional hydrogen bonds (see Tables 3−5 for more details). Therefore, the positive value of $\nabla^2\rho(r)$ for Au−X bond and negative value of $H(r)$ indicate that interaction of Au_3 cluster with active site of GSH ligand (Au−X, X = N, O, S) is partially covalent and partially electrostatic. However, positive values of both $\nabla^2\rho(r)$ and $H(r)$ indicate that interaction of Au_3 cluster with active site of GSH ligand (Au···H−X) is electrostatic in nature.

3.4. Natural Bond Orbital Analysis. NBOs[38] provide the most accurate possible (natural Lewis structure) picture of the wave function ψ because all the orbital details are mathematically chosen so as to include the highest possible percentage of the electron density. As a result, in the NBO analysis, the donor−acceptor (bond−antibond) interactions are taken into consideration by examining all possible interactions between "filled" (donor) Lewis-type NBOs and "empty" (acceptor) non-Lewis NBOs and then estimating their energies by second-order perturbation theory. These interactions (or energetic stabilizations) are referred to as "delocalization" corrections to the zeroth-order natural Lewis structure.

dx.doi.org/10.1021/jp2080226 | J. Phys. Chem. A 2012, 116, 4338−4347

Table 6. Charge Transfer Features of Neutral and Anionic GSH Complexes with the Au_3 Cluster Based on NBO Theory

complexes	interaction	ΔE_{CT}	complexes	interaction	ΔE_{CT}
GSH−Au_3(a)	$n_{N_5} \rightarrow \sigma^*_{O_1-H_1}$	12.4	GSH^-−Au_3(e)	$n_{O_3} \rightarrow \sigma^*_{O_1-H_1}$	7.3
	$n_{O_{15}} \rightarrow \sigma^*_{O_{20}-H_{20}}$	6.5		$n_{O_1} \rightarrow n^*_{Au1}(\alpha)$	27.2
	$n_{O_3} \rightarrow n^*_{Au_2}(\alpha)$	11.4		$n_{O_1} \rightarrow n^*_{Au_1}(\beta)$	29.3
	$n_{O_3} \rightarrow n^*_{Au_2}(\beta)$	23.7	GSH^-−Au_3(f)	$n_{O_3} \rightarrow \sigma^*_{O_1-H_1}$	15.5
	$n_{O_3} \rightarrow \sigma^*_{Au_2-Au_3}$	8.2		$n_{O_1} \rightarrow n^*_{Au_2}$	12.8
	$n_{Au_1} \rightarrow \sigma^*_{S_{13}-H_{13}}(\beta)$	5.5	GSH^-−Au_3(g)	$n_{O_1} \rightarrow \sigma^*_{O_{20}-H_{20}}$	12.3
GSH−Au_3(b)	$n_{N_5} \rightarrow \sigma^*_{O_1-H_1}$	9.7		$n_{O_1} \rightarrow \sigma^*_{N_{16}-H_{16}}$	2.2
	$n_{O_9} \rightarrow \sigma^*_{N_{16}-H_{16}}$	11.2		$n_{O_3} \rightarrow n^*_{Au_1}(\alpha)$	21.4
	$n_{O_3} \rightarrow \sigma^*_{N_{10}-H_{10}}$	8.7		$n_{O_3} \rightarrow n^*_{Au_1}(\beta)$	10.2
	$n_{O_{19}} \rightarrow n^*_{Au_2}(\alpha)$	12.5		$n_{Au_1} \rightarrow \sigma^*_{N_{10}-H_{10}}(\alpha)$	21.0
	$n_{O_{19}} \rightarrow n^*_{Au_2}(\beta)$	25.6	GSH^-−Au_3(h)	$n_{N_1} \rightarrow \sigma^*_{N_{10}-H_{10}}$	7.6
	$n_{O_{19}} \rightarrow \sigma^*_{Au_2-Au_3}$	5.7		$n_{O_{19}} \rightarrow \sigma^*_{N_5-H_5}$	28.0
GSH−Au_3(c)	$n_{N_5} \rightarrow \sigma^*_{O_1-H_1}$	10.1		$n_{O_{19}} \rightarrow \sigma^*_{N_5-H_5}$	2.4
	$n_{O_9} \rightarrow \sigma^*_{N_{16}-H_{16}}$	6.4		$n_{O_{19}} \rightarrow \sigma^*_{O_1-H_1}$	11.6
	$n_{O_3} \rightarrow \sigma^*_{N_{10}-H_{10}}$	6.9		$n_{O_{15}} \rightarrow n^*_{Au_1}(\alpha)$	16.7
	$n_{O_{15}} \rightarrow n^*_{Au_2}(\alpha)$	15.4		$n_{O_{15}} \rightarrow n^*_{Au_1}(\beta)$	46.4
	$n_{O_{15}} \rightarrow n^*_{Au_2}(\beta)$	44.9		$n_{O_{15}} \rightarrow \sigma^*_{Au_1-Au_2}$	6.2
	$n_{O_{20}} \rightarrow n^*_{Au_2}(\beta)$	4.5		$n_{O_{15}} \rightarrow \sigma^*_{Au_1-Au_3}$	4.3
	$n_{O_{15}} \rightarrow \sigma^*_{Au_1-Au_2}$	5.1	GSH^-−Au_3(i)	$n_{N_5} \rightarrow \sigma^*_{N_{10}-H_{10}}$	8.0
	$n_{O_{15}} \rightarrow \sigma^*_{Au_2-Au_3}$	5.3		$n_{O_{20}} \rightarrow \sigma^*_{O_1-H_1}(\alpha)$	11.6
	$n_{Au_1} \rightarrow \sigma^*_{O_{20}-H_{20}}(\alpha)$	12.9		$n_{O_{15}} \rightarrow \sigma^*_{Au_1-Au_2}$	12.6
GSH^-−Au_3(d)	$n_{O_1} \rightarrow \sigma^*_{N_5-H_5}$	5.0	GSH^-−Au_3(j)	$n_{N_5} \rightarrow \sigma^*_{N_{10}-H_{10}}$	11.7
	$n_{O_1} \rightarrow \sigma^*_{N_{10}-H_{10}}$	20.9		$n_{O_{19}} \rightarrow \sigma^*_{O_1-H_1}$	23.1
	$n_{S_{13}} \rightarrow n^*_{Au_1}(\alpha)$	4.8		$n_{S_{13}} \rightarrow n^*_{Au_1}$	5.2

The NBO analysis was performed here to deepen the nature of hydrogen bonds formed by the interaction of GSH with Au_3 cluster and to calculate charge transfer and Natural population analysis (NPA). In anchoring bonds Au−X (X = N, O, S), charge is transferred from the lone pair of nitrogen, oxygen, and sulfur to the σ^* and n^* orbitals of Au. In the nonconventional N−H···Au and O−H···Au hydrogen bonds, charge is transferred from the lone pair of Au to the σ^*_{N-H} and σ^*_{O-H} orbitals, respectively. In Table 6, the charge transfer energy values ΔE_{CT} between donor and acceptor orbitals within neutral and anionic complexes of GSH with Au_3 cluster are listed. These values have the same trends as binding energies (E_b). Generally, the lower orbital interaction energies of complexes of the Au_3 cluster with a GSH molecule imply less charge transfer and stronger ionic bond between Au_3 cluster and GSH molecule. The orbital interaction energies for intramolecular side chain hydrogen bonds in GSH ligand vary from 2.2 to 28.0 kcal/mol. As seen in Table 6 in all neural and anionic complexes of GSH with Au_3 cluster, the $n_X \rightarrow n^*_{Au}$ interaction participates in stabilization interaction, whereas in GSH−Au_3(b), GSH−Au_3(c), and GSH^-−Au_3(f) complexes, both $n_X \rightarrow n^*_{Au}$ and $n_{Au} \rightarrow \sigma^*_{X-H}$ interactions participate in the stabilization interaction between GSH and the gold cluster. Among $n_X \rightarrow n^*_{Au}$ charge transfer interactions, the strongest one belongs to $n_{O_{15}} \rightarrow n^*_{Au_1}(\beta)$ interaction in GSH^-−Au_3(j) (ΔE_{CT} = 46.4 kcal/mol), while strongest $n_{Au} \rightarrow \sigma^*_{X-H}$ charge transfer interactions belongs to $n_{Au_1} \rightarrow \sigma^*_{N10-H10}(\alpha)$ interaction in GSH^-−Au_3(f) (ΔE_{CT} = 21.0 kcal/mol).

Moreover, natural population analysis (NPA) was performed on optimized structures. Charge distributions of the active sites of GSH in neutral and anionic forms during an interaction with a Au_3 cluster are summarized in Table 7. In most of the complexes in which the Au_3 cluster interacts with GSH via the Au−X bond interaction type, the Au atom carries a positive charge and the X atom is partially negative, indicating that the Au−X interactions are electrostatic in nature, which has been confirmed by means of QTAIM analysis (as mentioned above).

Table 7. Calculated NPA Charges of Neutral and Anionic GSH Complexes with a Au_3 Cluster

complex	bond type	q_X[a]	q_{Au}	$\Delta q_{cluster}$[b]
GSH−Au(a)	Au_1···H_5	0.419	0.213	−0.105
	Au_2−O_3	−0.639	0.163	
GSH−Au(b)	Au_1···H_{13}	0.114	−0.178	−0.068
	Au_2−O_3	−0.690	0.151	
GSH−Au(c)	Au_1···H_{20}	0.509	−0.210	−0.064
	Au_2−O_{15}	−0.691	0.163	
GSH^-−Au(d)	Au_1−S_{13}	0.073	0.012	−0.285
GSH^-−Au(e)	Au_1···H_{13}	0.126	−0.178	−0.183
	Au_2−O_3	−0.765	0.117	
GSH^-−Au(f)	Au_1−O_3	−0.783	0.133	−0.202
GSH^-−Au(g)	Au_1−O_1	0.138	−0.840	−0.180
GSH^-−Au(i)	Au_1−O_{20}	−0.732	0.200	−0.193
GSH^-−Au(j)	Au_1−S_{13}	0.044	−0.022	−0.312
GSH^-−Au(h)	Au_1−O_{15}	−0.722	0.162	−0.155

[a] X = N, O, S, and H. [b] $\Delta q_{cluster} = q_{Au_3(complexed)} - q_{Au_3(isolated)}$.

dx.doi.org/10.1021/jp2080226 | J. Phys. Chem. A 2012, 116, 4338−4347

The charge differences in the Au_3 cluster, $\Delta q_{cluster} = q_{Au_3(complexed)} - q_{Au_3(isolated)}$ are negative, implying that the Au_3 cluster oxidizes the GSH ligand as a result of the interaction (see Table 7).

4. CONCLUSION

Interactions of glutathione (GSH) tripeptide (in neutral and anionic forms) with a gold cluster have been described in the geometrical and energetic aspects using the DFT-B3LYP approach with 6-31+G**-LANL2DZ mixed basis set. It is believed that anchoring bonds (Au−X, where X is N, O, and S atoms) and nonconventional hydrogen bonds (Au···X−H) to be responsible for the interparticle interaction of gold particles and GSH. The result of the calculation revealed that, among neutral and anionic forms of glutathione tripeptide, anionic ones exhibited the most tendencies to interact with the gold cluster. The quantum theories of atoms in molecules and natural bond orbital analysis have also been applied to understand the nature of the hydrogen bonding interaction in complexes. The result from NPA suggests that the Au_3 cluster oxidizes the GSH ligand as a result of the interaction.

Our theoretical results demonstrated that the interparticle hydrogen bonding depends on anionic or neutral forms of GSH (generated as pH changes). Consequently, in spite of the ability of thiol-containing biomolecules to form through a metal−sulfide interaction (such as the cysteine amino acid), the complexation behavior of a glutathione tripeptide is governed by its backbone intramolecular hydrogen bonding. This is rationalized by the different molecular shapes of the different ionic forms of GSH. The new insight into the pH and chemical tenability of the interparticle hydrogen bonding interaction of GSH on gold nanoparticles have implications to the exploitation of GSH-nanoparticle systems as fictional nanoprobes for biological detection and biosensors.

■ ASSOCIATED CONTENT

Supporting Information

Cartesian coordinates of all optimized structures used in this work. This material is available free of charge via the Internet at http://pubs.acs.org.

■ AUTHOR INFORMATION

Corresponding Author

*E-mail: fattahi@sharif.edu; jamshidi@ccerci.ac.ir.

Notes

The authors declare no competing financial interest.

■ ACKNOWLEDGMENTS

Support from Sharif University of Technology is gratefully acknowledged.

■ REFERENCES

(1) Wang, W.; Rusin, O.; Xu, X.; Kim, K. K.; Escobedo, J. O.; Fakayode, S. O.; Fletcher, K. A.; Lowry, M.; Schowalter, C. M.; Lawrence, C. M.; Fronczek, F. R.; Warner, I. M.; Strongin, R. M. *J. Am. Chem. Soc.* **2005**, *127*, 15949−15958.

(2) (a) Alivisatos, A. P.; Johnsson, K. P.; Peng, X.; Wilson, T. E.; Loweth, C. J.; Bruchez, M. P.; Schultz, P. G. *Nature* **1996**, *382*, 609−611. (b) Parak, W. J.; Gerion, D.; Pellegrino, T.; Zanchet, D.; Micheel, C.; Williams, S. C.; Boudreau, R.; Gros, M. A. L.; Larabell, C. A.; Alivisatos, A. P. *Nanotechnology* **2003**, *14*, 829−938.

(3) (a) Elghanian, R.; Storhoff, J. J.; Mucic, R. C.; Letsinger, R. L.; Mirkin, C. A. *Science* **1997**, *277*, 1078−1080. (b) Cao, Y. W. C.; Jin, R. C.; Mirkin, C. A. *Science* **2002**, *297*, 1536−1540.

(4) Park, H. Y.; Schadt, M. J.; Wang, L. Y.; Lim, I-I. S.; Njoki, P. N.; Kim, S. H.; Jang, M. Y.; Luo, J.; Zhong, C. J. *Langmuir* **2007**, *23*, 9050−9056.

(5) (a) Ni, J.; Lipert, R. J.; Dawson, G. B.; Porter, M. D. *Anal. Chem.* **1999**, *71*, 4903−4908. (b) Grubisha, D. S.; Lipert, R. J.; Park, H. Y.; Driskell, J.; Porter, M. D. *Anal. Chem.* **2003**, *75*, 5936−5943.

(6) Ghosh, P.; Han, G.; Erdogan, B.; Rosado, O.; Krovi, S. A.; Rotello, V. M. *Chem. Biol. Drug Des.* **2007**, *70*, 13−18.

(7) (a) Remacle, F.; Kryachko, E. S. *Chem. Phys. Lett.* **2005**, *404*, 142−149. (b) Remacle, F.; Kryachko, E. S. *Nano Lett.* **2005**, *5*, 735−739. (c) Remacle, F.; Kryachko, E. S. *J. Phys. Chem. B* **2005**, *109*, 22746−22757.

(8) Burda, C.; Chen, X.; Narayanan, R.; El-Sayed, M. A. *Chem. Rev.* **2005**, *105*, 1025−1102.

(9) Zhang, F. X.; Han, L.; Israel, L. B.; Daras, J. G.; Maye, M. M.; Ly, N. K.; Zhong, C. *J. Analyst* **2002**, *127*, 462−465.

(10) Sudeep, P. K.; Joseph, S. T. S.; Thomas, K. G. *J. Am. Chem. Soc.* **2005**, *127*, 6516−6517.

(11) Dickinson, D. A.; Forman, H. J. *Biochem. Pharmacol.* **2002**, *64*, 1019−1026.

(12) Meister, A.; Anderson, M. E. *Annu. Rev. Biochem.* **1983**, *52*, 711−760.

(13) Rabenstein, D. L.; Guevremont, R.; Evans, C. A.; Sigel, H. *Metal Ions in Biological Systems*; Dekker: New York, 1995; pp103−141 .

(14) Berg, J. M.; Tymoczko, J. L.; Stryer., L. *Biochemistry*; Freeman & Company: New York, 2002.

(15) Odriozola, I.; Loinaz, I.; Pomposo, J. A.; Grande, H. J. *J. Mater. Chem.* **2007**, *17*, 4843−4845.

(16) Bieri, M.; Burgi, T. *Langmuir* **2005**, *21*, 1354−1363.

(17) Tajc, S. G.; Tolbert, B. S.; Basavappa, R.; Miller, B. L. *J. Am. Chem. Soc.* **2004**, *126*, 10508−10509.

(18) Rabenstein, D. L. *J. Am. Chem. Soc.* **1973**, *95*, 2797−2803.

(19) Krezel, A.; Bal, W. *Acta Biochim. Pol.* **1999**, *46*, 567−580.

(20) Cheng, C. C.; Pai, C. H. *J. Inorg. Biochem.* **1998**, *71*, 109−113.

(21) Sudeep, P. K.; Joseph, S. T. S.; Thomas, K. G. *J. Am. Chem. Soc.* **2005**, *127*, 6516−6517.

(22) (a) Kou, X.; Zhang, S.; Yang, Z.; Tsung, C. K.; Stucky, G. D.; Sun, L.; Wang, J.; Yan, C. *J. Am. Chem. Soc.* **2007**, *129*, 6402−6404. (b) Zhang, S.; Kou, X.; Yang, Z.; Shi, Q.; Stucky, G. D.; Sun, L.; Wang, J.; Yan, C. *Chem. Commun.* **2007**, *47*, 1816−1818.

(23) Brelle, M. C.; Zhang, J. Z.; Nguyen, L.; Mehra, R. K. *J. Phys. Chem. A* **1999**, *103*, 10194−10201.

(24) (a) Schaaff, T. G.; Whetten, R. L. *J. Phys. Chem. B* **2000**, *104*, 2630−2641. (b) Schaaff, T. G.; Knight, G.; Shafigullin, M. N.; Borkman, R. F.; Whetten, R. L. *J. Phys. Chem. B* **1998**, *102*, 10643−10646.

(25) Negishi, Y.; Takasugi, Y.; Sato, S.; Yao, H.; Kimura, K.; Tsukuda, T. *J. Am. Chem. Soc.* **2004**, *126*, 6518−6519.

(26) Ackerson, C. J.; Sykes, M. T.; Kornberg, R. D. *Proc. Natl. Acad. Sci. U.S.A.* **2005**, *102*, 13383−13385.

(27) Li, T.; Park, H. G.; Lee, H. S.; Choi, S. H. *Nanotechnology* **2004**, *15*, 660−663.

(28) (a) Basu, S.; Ghosh, S. K.; Kundu, S.; Panigrahi, S.; Praharaj, S.; Pande, S.; Jana, S.; Pal, T. *J. Colloid Interface Sci.* **2007**, *313*, 724−734. (b) Basu, S.; Pal, T. J. *Nanosci. Nanotechnol.* **2007**, *7*, 1904−1910.

(29) Hong, R.; Han, G.; Fernandez, J. M.; Kim, B. J.; Forbes, N. S.; Rotello, V. M. *J. Am. Chem. Soc.* **2006**, *128*, 1078−1079.

(30) Gerdon, A. E.; Wright, D. W.; Cliffel, D. E. *Anal. Chem.* **2005**, *77*, 304−310.

(31) Hepel, M.; Tewksbury, E. *J. Electroanal. Chem.* **2003**, *552*, 291−305.

(32) Ali, E. M.; Zheng, Y.; Yu, H.; Ying, J. Y. *Anal. Chem.* **2007**, *79*, 9452−9458.

(33) (a) Bieri, M.; Burgi, T. *Langmuir* **2005**, *21*, 1354−1363. (b) Bieri, M.; Burgi, T. *J. Phys. Chem. B* **2005**, *109*, 10243−10250.

(c) Bieri, M.; Burgi, T. *J. Phys. Chem. B* **2005**, *109*, 22476−22485. (d) Bieri, M.; Burgi, T. *Phys. Chem. Chem. Phys.* **2006**, *8*, 513−520.
(34) Becke., A. D. *J. Chem. Phys.* **1993**, *98*, 5648−5652.
(35) Lee, C.; Yang, W.; Parr, R. G. *Phys. Rev. B* **1988**, *37*, 785−789.
(36) *Spartan*, Version 06V102; Wavefunction, Inc.: Irvine, CA, 2006.
(37) (a) Hay, P. J.; Wadt, W. R. *J. Chem. Phys. Chem.* **1985**, *82*, 270−283. (b) Hay, P. J.; Wadt, W. R. *J. Chem. Phys. Chem.* **1985**, *82*, 284−298. (c) Hay, P. J.; Wadt, W. R. *J. Chem. Phys. Chem.* **1985**, *82*, 299−310.
(38) Reed, A. E.; Curtiss, L. A.; Weinhold, F. *Chem. Rev.* **1988**, *88*, 899−926.
(39) Glendening, E. D.; Badenhoop, J. K.; Reed, A. E.; Carpenter, J. E.; Bohmann, J. A.; Morales, C. M.; Weinhold, F. *GEN NBO 5.0*; Board of Regents of the University of Wisconsin System on behalf of the Theoretical Chemistry Institute: Madison, WI, 2001.
(40) Bader, R. F. W. *Atoms in Molecules. A Quantum Theory*; Clarendon: Oxford, U.K., 1990; pp 188−250.
(41) Bader, R. F. W. *AIM2000 Program Package*, Version 2.0; McMaster University: Hamilton, Ontario, Canada, 2002.
(42) Desfrancüois, C.; Carles, S.; Schermann, J. P. *Chem. Rev.* **2000**, *100*, 3943−3962.
(43) Pakiari, A. H.; Jamshidi, Z. *J. Phys. Chem. A* **2007**, *111*, 4391−4396.
(44) Popelier, P. L. A. *Atoms in Molecules: An Introduction*; Prentice Hall: London, 2000; pp 100−188.
(45) Cremer, D.; Kraka, E. *Angew. Chem.* **1984**, *23*, 627−628.
(46) Koch, U.; Popelier, P. L. A. *J. Phys. Chem.* **1995**, *99*, 9747−9754.